
Deep Multivariate Models with Parametric Conditionals

Dmitrij Schlesinger¹ Boris Flach² Alexander Shekhovtsov²

Abstract

We consider deep multivariate models for heterogeneous collections of random variables. In the context of computer vision, such collections may e.g. consist of images, segmentations, image attributes, and latent variables. When developing such models, most existing works start from an application task and design the model components and their dependencies to meet the needs of the chosen task. This has the disadvantage of limiting the applicability of the resulting model for other downstream tasks. Here, instead, we propose to represent the joint probability distribution by means of conditional probability distributions for each group of variables conditioned on the rest. Such models can then be used for practically any possible downstream task. Their learning can be approached as training a parametrised Markov chain kernel by maximising the data likelihood of its limiting distribution. This has the additional advantage of allowing a wide range of semi-supervised learning scenarios.

1. Introduction

When modelling joint probability distributions, say $p(x, y)$, in terms of deep networks, usually, the first question is how to factorise it, i.e. to decompose it into parts which are then modelled by deep networks. The choice of this decomposition is almost always dictated by the intended inference problem. For example, if x is observable, y is a class label, and the intended task is classification, the appropriate factorisation is $p(x, y) = p(x)p(y | x)$. If, on the other hand, the intended task is conditional generation, the reverse factorisation $p(x, y) = p(y)p(x | y)$ is suitable. The crucial point is that there is no single factorisation that enables solving both inference problems. If e.g. $p(x | y)$ is modelled in terms of a deep network, the reverse conditional $p(y | x)$ is not accessible even in the case of a simple model

¹Dresden University of Technology ²Czech Technical University in Prague. Correspondence to: Dmitrij Schlesinger <dmytro.shlezinger@tu-dresden.de>.

for $p(y)$.

The issue becomes even more difficult for more than two variables, e.g. $p(x, y, z)$, because the number of possible factorisations grows exponentially with the number of variables. Moreover, a particular factorisation admits only a few inference problems. For example, the factorisation $p(x, y, z) = p(x)p(y | x)p(z | x, y)$ admits predicting y from x , but not y from x and z . Performing the latter requires the conditional $p(y | x, z)$, which is not directly modelled in the chosen factorisation. Its computation from the learned factors is usually infeasible if the latter are modelled by complex deep networks. A typical example is variational autoencoders (VAE) (Kingma & Welling, 2014; Rezende et al., 2014) and conditional VAEs (Sohn et al., 2015; Kingma et al., 2014). They establish a (statistical) relation between images, classes and latent variables by choosing a factorisation suitable for the respective main goal (e.g. semi-supervised model learning for conditional generation and inference). Tasks that are not directly accessible by the chosen model factorisation are then delegated to auxiliary encoders, which are used for lower bounding the training objective without being part of the model. This has the disadvantage that they are not consistent with the model and often require additional terms in the learning objective.

Our main desiderata are therefore to model complex multivariate joint probability distributions such that they can be (i) used for various downstream inference tasks and (ii) trained with arbitrary levels of supervision. For this, we propose to represent joint probability distributions by means of conditional probability distributions for each group of variables conditioned on the rest. For the example above, we would represent $p(x, y, z)$ by means of three conditionals $p(x | y, z)$, $p(y | x, z)$ and $p(z | x, y)$. The joint distribution $p(x, y, z)$ is then defined as the limiting distribution of an MCMC process that alternately samples from the given conditionals. We propose an algorithm that learns the conditional distributions by maximising the data likelihood of the limiting distribution while encouraging them to be consistent with each other. Inference according to any conditional distribution, e.g. $p(x | y)$, becomes accessible via the MCMC process with clamped inputs.

The rest of the paper is organised as follows. Section 2 reviews the related work. In Section 3 we consider learning

limiting distributions defined by parametrised MCMC transition probabilities in a general setting, without partitioning variables into groups, and propose a recurrent lower bound approach. Section 4 details the approach for the case of multivariate joint probability distributions, shows a connection between consistency and detailed balance, and proposes a learning algorithm applicable with arbitrary levels of supervision. The experimental Section 5 validates the properties of the learning algorithm and proposes proof-of-concept experiments in semi-supervised learning and multiple direction inference on vision-related datasets.

2. Related Work

We develop the idea of specifying a joint distribution by its conditionals. In the context of VAEs, the decoder $p(x|z)$ and encoder $q(z|x)$ may be *consistent*, i.e. true conditionals of some joint distribution $p(x,z)$, implicitly defined in this way. The prior $p(z)$ is then already implied by the joint. An explicitly specified simple $p(z)$ imposes an additional constraint. Towards closing this discrepancy, Tomczak & Welling (2018) proposed VampPrior, defined with the help of the encoder, and showed that it is beneficial for generative capabilities and a better latent structure. On the other hand, if the encoder and decoder are in exponential families — a common choice in VAEs, then only RBM-like joint distributions may satisfy consistency (Arnold & Strauss, 1991; Arnold et al., 2001; Shekhovtsov et al., 2022). Liu et al. (2021) circumvent this issue by using a flow-based model for the encoder and propose a consistency-enforcing loss as well as ways to sample from model marginals *assuming that consistency holds*. However, their approach is only applicable in the bivariate case. We propose instead learning the limiting distribution specified by conditional models. To do this, we construct a lower bound on the likelihood target that implicitly enforces consistency. The resulting approach generalises well to the multivariate case. We expect that multivariate models with more variables, in particular hierarchical, can combine consistency with expressive power. Unlike Liu et al. (2021), our approach is applicable in such cases.

Flach et al. (2024) circumvent the consistency of VAE (with or without prior) by formulating the learning as a two-player game between an encoder and decoder. In the simple case of unsupervised learning, this leads to the wake-sleep algorithm (Hinton et al., 1995). Our Algorithm 1 is a generalisation: it recovers these previous algorithms in the case of two variables when terminating the MCMC chain at length 1. The chain length allows for balancing consistency vs likelihood trade-off, previously possible only with more complex approaches (Liu et al., 2021).

Lamb et al. (2017) also consider learning a limiting distribution of a Markov Chain cycling through conditionals, called

GibbsNet. Their training approach is, however, different from ours: using a GAN, it matches the limiting joint distribution to the distribution obtained by clamping the observed variables to the data distribution. They claim that it can, in principle, be applied to solve multiple inference tasks and admits semi-supervised learning. However, both the analysis and experiments are limited to just two groups of variables: observed and latent.

3. Learning Limiting Distributions

Let $p_\theta(x|x')$, $\theta \in \Theta$, $x, x' \in \mathcal{X}$, be a parameterised transition probability matrix defining a Markov chain with a possibly large but finite state space \mathcal{X} . We assume that it has a unique limiting distribution¹ denoted by $p_\theta(x)$. Given a data distribution $q(x)$, we want to train the implicit model $p_\theta(x)$ by maximising the likelihood

$$L(\theta) = \sum_{x \in \mathcal{X}} q(x) \log p_\theta(x) \rightarrow \max_{\theta \in \Theta}. \quad (1)$$

We assume that sampling from $p_\theta(x|x')$ and computing its derivative w.r.t. θ are both possible. However, this does not yet allow us to maximise the objective $L(\theta)$ directly. To approach the task, we propose to use a lower bound similar to variational inference.

Let $q(x|x')$ be another Markov chain model on \mathcal{X} with a unique limiting distribution. Starting from the given data distribution, i.e. $q_1(x) := q(x)$, we define the following two sequences of distributions $q_k(x)$ and $Q_k(x)$, $k = 2, 3, \dots$ recursively:

$$q_k(x) = \sum_{x' \in \mathcal{X}} q(x|x')q_{k-1}(x') \quad (2a)$$

$$Q_n(x) = \frac{1}{n} \sum_{k=1}^n q_k(x). \quad (2b)$$

Both sequences converge to the unique limiting distribution of the model $q(x|x')$. Using the *stationarity condition* $p_\theta(x) = \sum_{x'} p_\theta(x')p_\theta(x|x')$ for the limiting distribution $p_\theta(x)$, we can expand and lower bound $L(\theta)$ as follows:

$$\begin{aligned} L(\theta) &= \sum_{x \in \mathcal{X}} q_1(x) \log \sum_{x' \in \mathcal{X}} p_\theta(x|x')p_\theta(x') \geqslant \\ L_B(\theta, q) &= \sum_{x \in \mathcal{X}} q_2(x) \log p_\theta(x) + \\ &\quad \sum_{x, x' \in \mathcal{X}} q(x'|x)q_1(x) \left[\log p_\theta(x|x') - \log q(x'|x) \right]. \end{aligned} \quad (3)$$

Repeating this step for the first term of $L_B(\theta, q)$ recursively,

¹I.e. when some power of the transition probability matrix is strictly positive.

we obtain an n 'th-order lower bound

$$L_B(\theta, q, n) = \sum_{x \in \mathcal{X}} q_{n+1}(x) \log p_\theta(x) + \sum_{x, x' \in \mathcal{X}} q(x' | x) Q_n(x) \left[\log p_\theta(x | x') - \log q(x' | x) \right]. \quad (4)$$

To analyse this lower bound, we use the following reformulation.

Proposition 3.1. *The lower bound (4) has an equivalent reformulation $L_B(\theta, q, n) =$*

$$L(\theta) - n \sum_{x \in \mathcal{X}} Q_n(x) D_{KL}(q(x' | x) \| p_\theta^r(x' | x)), \quad (5)$$

where $p_\theta^r(x' | x) = p_\theta(x | x') p_\theta(x') / p_\theta(x)$ is the transition kernel of the reverse Markov chain.

This shows that $L_B(\theta, q, n)$ is tight iff $q(x' | x)$ coincides with the reverse model $p_\theta^r(x' | x)$.

We would like to approach maximising $L_B(\theta, q, n)$ by a generalised EM algorithm, improving $L_B(\theta, q, n)$ in θ for a fixed q in one iteration and updating q to make the bound tighter in the other. Computing the gradient of the lower bound is, however, no simpler than computing the gradient of the likelihood $L(\theta)$ because the first term of (4) involves the limiting distribution $p_\theta(x)$. The next proposition shows that this term can be omitted for large n .

Proposition 3.2. *Let $q(x' | x)$ be such that its unique limiting distribution coincides with $p_{\bar{\theta}}(x)$ for a given fixed $\bar{\theta}$. Then the gradient of the first term of (4) in θ at $\bar{\theta}$ asymptotically vanishes for $n \rightarrow \infty$. In particular, it holds that $\|\nabla_\theta \sum_{x \in \mathcal{X}} q_n(x) \log p_\theta(x)\|_1 \leq C\alpha^n$ with some $\alpha \in (0, 1)$ related to the mixing time of the kernel $q(x' | x)$ and a positive constant C .*

This motivates the following generic learning algorithm, ignoring the first term of (4) and estimating the gradient of the second term of (4) stochastically, i.e. by sampling from q and differentiating $p_\theta(x | x')$:

1. For the current parameter $\theta^{(t)}$ chose $q^{(t)}(x' | x)$ with limiting distribution $p_{\theta^{(t)}}(x)$.
2. Use $q^{(t)}$ to sample a sequence (x_1, \dots, x_{n+1}) starting from $x_1 \sim q(x)$ – the data distribution.
3. Estimate the gradient of $L_B(\theta, q^{(t)}, n)$ as

$$g = \sum_{k=1}^n \nabla_\theta \log p_\theta(x_k | x_{k+1}). \quad (6)$$

4. Update $\theta^{(t+1)} = \theta^{(t)} + \lambda g$, where λ is the learning rate.

The proofs of the two propositions and further facts used for this algorithm can be found in Section A.1.

The algorithm becomes particularly sound when it is possible to use $q^{(t)}(x' | x) = p_{\theta^{(t)}}^r(x' | x)$, i.e. when sampling from the reverse chain is feasible. In particular, this is the case when $p_\theta(x' | x)$ satisfies detailed balance². If we use $q^{(t)}(x | x') = p_{\theta^{(t)}}^r(x | x')$ in the algorithm, the lower bound $L_B(\theta, q^{(t)}, n)$ becomes tight at $\theta^{(t)}$ and its gradient coincides with the gradient of the likelihood $L(\theta)$ at $\theta^{(t)}$, for any n . This choice of q also satisfies Proposition 3.2 because the limiting distribution of the reverse chain is the same as the limiting distribution of the forward chain.

However, the accessibility of the reverse model is a rather limiting assumption, not satisfied in particular when the kernel $p_\theta(x | x')$ is modelled with deep networks, which is of central interest in this work. Instead, we propose reusing the forward model $p_{\theta^{(t)}}(x' | x)$ for q . In this case, $L_B(\theta, q^{(t)}, n)$ is not tight but is still a valid lower bound to maximise. Moreover, Proposition 3.2 still applies for this choice. We analyse the behaviour of the algorithm with this choice, assuming that the family of models $p_\theta(x | x')$, $\theta \in \Theta$ is rich enough to combine expressive power with detailed balance, i.e. contains a large subset $\Theta_{DB} \subset \Theta$ of models satisfying detailed balance.

We conjecture that the algorithm implies a bias towards detailed balance. As we discussed, up to the omitted term with vanishing gradient for $n \rightarrow \infty$, the algorithm can be interpreted as stochastic gradient ascent for (5). Thus, at each iteration, it balances between maximising the likelihood $L(\theta)$ and minimising the KL divergence from $q(x' | x) = p_\theta(x' | x)$ to $p_\theta^r(x' | x)$, enforcing their equality, i.e. the detailed balance. The KL divergence has a weight of n in (5). Therefore, the larger n , the stronger the force towards the detailed balance. The KL term and its gradient vanish only if $\theta \in \Theta_{DB}$. If this happens, we are effectively able to sample from the reverse chain correctly, and the algorithm's behaviour can be expected to follow the preceding case.

To summarise, we expect the algorithm with $q^{(t)}(x' | x) = p_{\theta^{(t)}}(x' | x)$ and large n to seek a maximum likelihood solution amongst models satisfying detailed balance. In the case when the set Θ_{DB} is not rich enough, we have to use a smaller n to allow for a reasonable trade-off between detailed balance and likelihood. However, choosing a smaller n might impair the accuracy of gradient approximation. It is then up to the experiments to verify whether this trade-off still leads to useful models.

Remark 3.3. We strongly believe that all derivations extend to continuous state spaces \mathcal{X} . The only limitation is guaranteeing the uniqueness of the limiting distribution that needs to be assumed for the entire model family.

Remark 3.4. It is noteworthy that choosing an aux-

²The Markov chain satisfies detailed balance, if the reverse model coincides with the forward model.

iliary model $q(x|x')$ with positive KL-divergence $D_{KL}(q(x'|x) \parallel p_\theta(x'|x))$ has the consequence that the gap between the likelihood and the lower bound (5) grows approximately linearly in n . Interestingly, this does not necessarily lead to a breakdown of the approach. A prominent example is denoising diffusion (Ho et al., 2020; Rombach et al., 2022) (see Example 1 in Appendix A.3).

4. Multivariate Models with Parametric Conditionals

As mentioned in the introduction, our central goal is to develop and learn deep multivariate models for heterogeneous collections of random variables. Let $x = (x_1, x_2 \dots x_m)$ be a collection of such heterogeneous random variables³. Let $p_{\theta_i}(x_i | x_{-i})$, for $i = 1 \dots m$, be a conditional probability distribution for each variable x_i conditioned on all other variables and parametrised by its own parameter θ_i . We consider an MCMC process that alternates between sampling components x_i . The joint Markov kernel of this MCMC process can be formally written as a convex combination

$$p_\theta(x | x') = \sum_{i=1}^m \alpha_i p_{\theta_i}(x_i | x_{-i}) \llbracket x_{-i} = x'_{-i} \rrbracket \quad (7)$$

where the indicator $\llbracket x_{-i} = x'_{-i} \rrbracket$ expresses that all variables except x_i remain unchanged and α_i defines the relative frequency of resampling of each component. This process is similar to Gibbs sampling and allows addressing multiple inference problems by clamping the subset of observed variables x_o and iteratively resampling the rest. Supervised learning of $\{\theta_i\}$ is possible via the methods of Section 3 and semi-supervised learning becomes possible by the expectation-maximisation principle, first completing missing parts of a training example according to the current model.

In the above outline, there is the following subtlety: if $\{\theta_i\}$ are arbitrary, differently clamped processes may be inconsistent. To formalise this, assume that the process with kernel (7) has a unique limiting distribution $p_\theta(x)$. The question is whether the MCMC process with clamped x_o will have the same limiting distribution as $p_\theta(x_{-o} | x_o)$ implied by $p_\theta(x)$. This will be the case when model conditionals are consistent, as we now explain.

Definition 4.1. A collection of conditional distributions $p_{\theta_i}(x_i | x_{-i})$, $i = 1, \dots, m$ is *consistent* if there exists a joint distribution $p(x)$ that has them as conditionals.

One example of a consistent system of conditionals is the EF-Harmonium (Welling et al., 2004), a generalisation of RBM (which we will consider in Example 3 in Appendix A.3). Arnold et al. (2001); Shekhovtsov et al. (2022)

³Here, we use lower indices to denote components in contrast to the previous section, where they were denoting time steps.

Algorithm 1: Learning Joint Probability Distributions

Input: training example (x_o, x_{-o}) , where x_o is the group of observed and x_{-o} is the group of unobserved variables; conditional probability distributions $p_{\theta_i}(x_i | x_{-i})$ for each variable.

I. Complete the example by sampling over unobserved variables:

```
Initialise  $\hat{x} = (x_o, \hat{x}_{-o})$  with random  $\hat{x}_{-o}$ 
repeat  $n_{\text{inference}}$  times
    Randomly choose unobserved  $i \in -o$ 
    Draw  $\hat{x}_i \sim p_{\theta_i}(x_i | \hat{x}_{-i})$ 
```

II. Learn the model on the completed example \hat{x} :

```
repeat  $n$  times
    Randomly choose a component  $i \in \{1, \dots, m\}$ 
    Compute  $g \leftarrow \nabla_{\theta_i} \log p_{\theta_i}(\hat{x}_i | \hat{x}_{-i})$ 
    Update  $\theta_i \leftarrow \theta_i + \lambda g$ 
    Draw  $\hat{x}_i \sim p_{\theta_i}(x_i | \hat{x}_{-i})$ 
```

discuss such consistency for the case of two variates. We note that if $p_{\theta_i}(x_i | x_{-i})$ are consistent, then an MCMC process with clamped x_o becomes a Gibbs sampling scheme, guaranteed to sample from $p_\theta(x_{-o} | x_o)$. We further characterise this consistency in terms of detailed balance of the Markov chain.

Theorem 4.2. *The Markov chain defined by the kernel (7) satisfies detailed balance if and only if the collection of conditional distributions $p_{\theta_i}(x_i | x_{-i})$, $i = 1, \dots, m$ is consistent. In this case, all individually modelled conditionals $p_{\theta_i}(x_i | x_{-i})$ coincide with the corresponding conditionals of the limiting distribution, $p_\theta(x_i | x_{-i})$.*

The proof is given in Appendix A.2. We see that the detailed balance of the Markov chain, which was desirable for learning in Section 3, is also necessary for rigorous inference with the proposed method. As we have argued, the generic algorithm (6) with the choice $q(x | x') = p_\theta(x | x')$ enforces detailed balance. The theorem implies that it also enforces consistency when applied to multivariate models; therefore, the choice $q(x | x') = p_\theta(x | x')$ is of particular interest. Next, we discuss semi-supervised learning cases.

Practical Learning Algorithm Without loss of generality, training examples can be assumed to have an observed part x_o and an unobserved part x_{-o} . This partitioning can be different for different examples, but it is considered to be independent of the data itself. The likelihood of the observed part is given by

$$\log p_\theta(x_o) = \log \sum_{x_{-o}} p_\theta(x_o, x_{-o}). \quad (8)$$

Following the expectation-maximisation scheme, we use a stochastic approximation of its gradient

$$\hat{x}_{-o} \sim p_{\theta(t)}(x_{-o} | x_o), \quad (9a)$$

$$\nabla_{\theta} \log p_{\theta}(x_o) \approx \nabla_{\theta} \log p_{\theta}(x_o, \hat{x}_{-o}), \quad (9b)$$

i.e., we first complete the example by sampling the missing values from $p_{\theta(t)}(x_{-o} | x_o)$, according to the current model $\theta^{(t)}$. This is achieved by running the sampler (7) with clamped values x_o and is implemented in step I of Algorithm 1. The required number of repeats, $n_{\text{inference}}$, depends on the mixing time of the sampler (7). The same holds for the inference when we observe x_o and want to predict x_{-o} . Completed examples proceed to step II, implementing the method of Section 3 for $q(x | x') = p_{\theta}(x | x')$.

Instead of generating a chain of length n for each individual training example, in step II we keep a batch of examples and in each iteration update the model parameters and resample all examples in the batch according to the transition kernel. In the actual implementation, we also replace a fraction of examples at random with fresh ones from the training data (suitably completed with step I). This way, the loop in step II can run continuously, with the chain for each example having some probability to terminate when it is replaced with a fresh one. We observed this to improve stability. As a consequence, in practice, we do not have an explicit chain length hyperparameter n but an *expected chain length*, defined by the batch size and the replacement ratio.

Remark 4.3. The chain length n (or the equivalent expected chain length) has multiple effects: 1) Training time. 2) A larger n is needed for the approximation used in Proposition 3.2, especially for models with a large mixing time. 3) In practical situations, when conditionals $p_{\theta_i}(x_i | x_{-i})$ are not flexible enough to ensure consistency (e.g. simple exponential families such as factorised Gaussian or Bernoulli), a lower n needs to be used according to the trade-off (5); otherwise, the gradient of the consistency-enforcing term is much larger than that of the likelihood. Currently, we do not have control over the mixing time and focus on the training methodology and proof-of-concept experiments, demonstrating that useful trade-offs do exist.

5. Experiments

5.1. Validation: Learning Consistency

In this experiment, we demonstrate, on a toy example, that the proposed algorithm can learn the true joint distribution, even if some training data are incomplete. We consider $z \in \{0, 1\}^3$ and a ground-truth distribution $p^*(z) \propto \exp(a \sum_i z_i + b \sum_{i < j} z_i z_j)$, i.e. a homogeneous Ising model on a complete graph with three nodes. The learned model consists of three conditional distributions implemented as MLPs. It was trained by our approach in

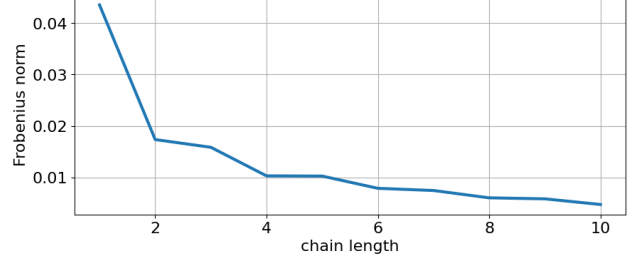


Figure 1. Artificial experiment: dependency of the matrix asymmetry on the chain length n .

two variants: (1) Using complete data generated from p^* and (2) Using data generated from p^* with components missing at random. The approximation quality was measured by the KL-divergence of the limiting distribution from the ground-truth model. We repeated each experiment 100 times. The average KL-divergence and the standard deviation were: 0.0007 ± 0.0004 in the first experiment and 0.0018 ± 0.0013 in the second one. We believe this shows that the proposed approach works as expected, including also semi-supervised learning.

5.2. Validation: Chain Length

This experiment investigates the behaviour of the algorithm proposed in Section 3 in the non-tight case with $q(x' | x) = p_{\theta}(x' | x)$ and aims to confirm its bias towards detailed balance. We learn a simple log-linear transition probability distribution to match a given target distribution. Let $z \in \{-1, +1\}^n$ be a vector of binary variables (we use $n=64$ in this experiment), and $\pi(z) := q_1(z)$ be the target probability distribution. The transition probability distribution is defined as

$$p_{\theta}(z_t | z_{t-1}) \propto \exp\langle W z_{t-1} + b, z_t \rangle, \quad (10)$$

where the matrix $W \in \mathbb{R}^{n \times n}$ and the bias $b \in \mathbb{R}^n$ are unknown parameters, summarised by θ . We use the marginal distribution of the latent variables $p(z)$ from our MNIST experiments as the target probability distribution $\pi(z)$ (see Section 5.3 and Section B for details).

We notice that the model satisfies detailed balance $p_{\theta} = p_{\theta}^r$ iff W is symmetric. The asymmetry of W , measured with Frobenius norm $\|W - W^T\|_F$, can therefore serve as a natural measure for detailed balance. We perform a series of experiments varying the chain length n . Figure 1 shows the dependency of the resulting matrix's asymmetry on the chain length. As expected, the learned matrix W becomes symmetric for longer chains. This confirms our conjecture that the algorithm implicitly enforces detailed balance, which tightens the lower bound, making it closer to the likelihood. Additional details and further experiments accomplishing these results can be found in Section B.

5.3. MNIST / Fashion MNIST

This experiment illustrates our approach on simple labelled image data. The task is to learn a distribution $p(x, c)$, where x are images and c are classes. In particular, for MNIST, we consider binarised images $x \in \mathcal{B}^{28 \times 28}$ (a common simplification) and classes $c \in \mathcal{C} = \{0, 1, \dots, 9\}$ corresponding to digits. We introduce additional latent variables $z \in \mathcal{B}^m$ (we used $m=64$), which should “encode” different appearances for each symbol. Hence, the full joint model is $p(x, c, z)$. It is specified by means of the following three conditional probability distributions:

$$\begin{aligned} p(x | c, z) &\propto \exp\langle f_x(c_{oh}, z), x \rangle, \\ p(c | x, z) &\propto \exp\langle f_c(x) + z^T W_c, c_{oh} \rangle, \\ p(z | x, c) &\propto \exp\langle f_z(x) + c_{oh}^T W_z, z \rangle, \end{aligned} \quad (11)$$

where c_{oh} is one-hot encoded c . The functions $f_c: \mathcal{X} \rightarrow \mathbb{R}^{10}$ and $f_z: \mathcal{X} \rightarrow \mathbb{R}^m$ are convolutional feedforward networks with an encoder-like architecture, i.e. with decreasing spatial resolution. The decoder $f_x: \mathcal{B}^{10+m} \rightarrow \mathbb{R}^{28 \times 28}$ (c_{oh} and z are concatenated) consists of a few “transposed convolutional” layers, W_c and W_z are $m \times 10$ and $10 \times m$ matrices, respectively.

The model for Fashion MNIST is exactly the same except that we use grey-valued images $x \in \mathbb{R}^{28 \times 28}$ and model $p(x | c, z)$ as a Gaussian $p(x | c, z) = \mathcal{N}(x; \mu(c, z), \sigma)$, where the means $\mu(c, z)$ for each pixel are provided by a feedforward network with the same architecture as f_x in (11) and $\sigma \in \mathbb{R}$ is a global learnable parameter. In addition, we increased the dimension of the latent space from $m = 64$ to $m = 256$.

The models were learned by Algorithm 1. The completion step I in these models is trivial – for each training sample, we only need to sample once from $p(z | x, c)$. The optimisation step II of the algorithm was performed with the average chain length $n = 4$.

The results of conditional generation are presented in Figure 2. Given a class c , we sample images $x \sim p(x | c)$, which can be done by alternately sampling from $p(x | c, z)$ and $p(z | x, c)$, starting from a random z . For better visualisation, we show probabilities $p(x | c, z)$ for MNIST and means $\mu(c, z)$ for Fashion MNIST for the last sampled z . In order to rate the image quality quantitatively, we use the Fréchet Inception Distance (we used the code from (Seitzer, 2020)). The obtained values are 5.87 for MNIST and 30.49 for Fashion MNIST.

Next, we define a classification task as maximum marginal decision $\arg \max_c \sum_z p(c, z | x)$, where marginalisation over z is implemented by alternating sampling from $p(c | x, z)$ and from $p(z | x, c)$, starting from a random z . We achieve 99.04% classification accuracy on MNIST and 88.61% on Fashion MNIST.



Figure 2. Conditional generation for MNIST / Fashion MNIST. Columns correspond to classes.

The achieved values are on par with or slightly worse than the actual state-of-the-art⁴. The aim of the experiment was rather to illustrate the “universality” of our approach, i.e. using one and the same model for different inference problems. We have not tuned the models towards a specific inference problem. Nevertheless, we find that the same simple model architecture works quite well for different datasets.

5.4. CelebA

The next group of experiments illustrates our approach on more challenging data. We use the CelebA-HQ dataset, containing images of human faces, along with attributes and segmentations. In particular, we demonstrate the ability of our approach to cope with different downstream tasks.

We introduce the following random variables. Let $x \in \mathbb{R}^{3 \times 64 \times 64}$ be images (we downsampled images and segmentations to 64×64 resolution for simplicity), $s \in \mathcal{B}^{18 \times 64 \times 64}$ be segmentations (a binary mask for each of the 18 segments) and $c \in \mathcal{B}^{40}$ be image attributes, like e.g. “male”, “blond”, “wearing glasses”, etc. In addition, we introduce two groups of latent variables: $y \in \mathcal{B}^{256}$ are binary and $z \in \mathbb{R}^{16}$ are continuous.

The joint model is represented by five conditional probability distributions, i.e. for each variable conditioned on the rest. Each conditional is implemented as a feed-forward network of moderate complexity. Thereby, networks for binary variables output logits, whereas networks for continuous variables x and z output means and variances for each element, for example $p(x | c, y, z, s) =$

⁴We used <https://paperswithcode.com> to get an overview.

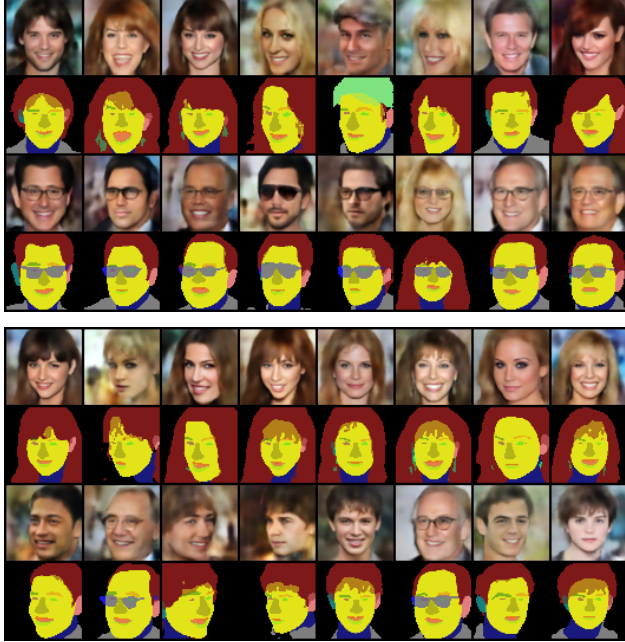


Figure 3. Generation for CelebA, conditioned on the presence of glasses attribute (top) and male attribute (bottom). Each display shows pairs of image and segmentation generated with the attribute switched off (first two rows) and switched on (last two rows).

$$\mathcal{N}(x; \mu(c, y, z, s), \sigma(c, y, z, s)).$$

The model was learned by the Algorithm 1 for about 470k gradient updates (corresponding to 1000 epochs in our implementation). We used 10 sampling iterations in the completion step I (we need to complete triples (c, x, s) by sampling the latent variables y and z) and the expected chain length $n = 16$ in step II. Further details are given in Section C. In Figure 3 we demonstrate generation conditioned on attributes. The achieved FID score for the generated images is 46.45.

The next experiment demonstrates the ability of the learned model to complete missing information for any subset of its variables, including any subset of their individual coordinates. This problem cannot be approached by any standard factorisation, because the subset of unobserved variables is not known at training time. We illustrate this ability on the example of segmentation from incomplete images. Let $x = (x_o, x_h)$, where the part x_o is observed and x_h is hidden. In order to segment such an image by the maximum marginal decision strategy, we need to compute the marginal probabilities $p(s_{ik} | x_o)$ for each pixel i and segmentation label k . They can be estimated by sampling, which alternately draws all unobserved random variables, including x_h , while clamping x_o . We accumulate segmentation label frequencies for each pixel during the sampling and finally set the label k if its marginal probability is greater than 0.5. At the same time, we complete the missing image content (i.e.

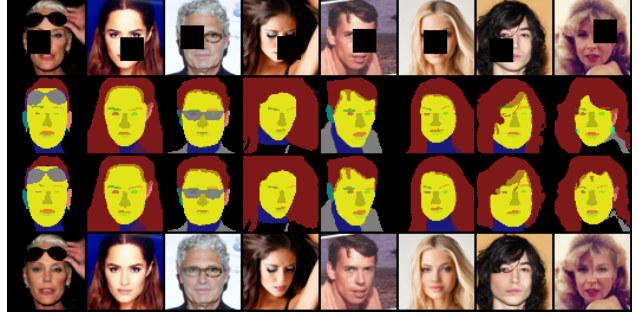


Figure 4. Segmentation from incomplete images / in-painting. First row: original images with hidden parts shown as black squares, second row: ground truth segmentations, third row: predicted segmentations, fourth row: in-painting.



Figure 5. Image demixing. First two rows: original image pairs, third row: mixed image, last two rows: demixing results.

in-painting). For this, we employ a mean marginal decision, i.e. we average all sampled image values observed during sampling. The results are illustrated in Figure 4.

The final experiment shows how to extend the model to perform even more complex inference problems. We consider the following image “demixing” task. A mixed image x is obtained from two images x' and x'' by randomly choosing the RGB values in each pixel of x from either the first or the second image. The task is to reconstruct the original images given the mixed one.

In order to define an appropriate statistical model for this task, we consider two instances of our trained model for the random variables (c', x', y', z', s') and $(c'', x'', y'', z'', s'')$ for the first and the second image, respectively. In addition, we define a binary mask $m \in \mathcal{B}^{64*64}$ and assume a uniform prior $p(m)$. The mixed image is obtained as $x = x'*(1-m) + x''*m$. Even though the last expression is deterministic, it is easy to see how to sample all introduced components conditioned on x . For segmentations, attributes and latent variables, we can directly use the learned conditionals. In order to sample e.g. from $p(x' | c', y', z', s', x, m)$, we proceed as follows. We first sample from the learned

Table 1. FID scores for compared methods.

DATASET / METHOD	RANDOM CODE	LIMITING
FMNIST, VAE	81.70	52.66
FMNIST, SYMMETRIC	52.39	47.24
FMNIST, OUR	–	35.87
CELEBA, VAE	86.55	133.31
CELEBA, SYMMETRIC	98.97	120.65
CELEBA, OUR	–	118.92

conditional $p(x' | c', y', z', s')$, and then replace x' by x in pixels with $m = 0$ (similarly for x''). Finally, in order to sample from $p(m | \text{everything})$, we compute the likelihood ratio $\ln p(x | c'', y'', z'', s'') - \ln p(x | c', y', z', s')$, which is the logit for $p(m | \text{everything})$. We notice that this demixing task is highly ambiguous. Therefore, to regularise and simplify it, we assume known segmentations s' and s'' . Figure 5 shows the results.

5.5. Comparison to Other Methods

We compare the proposed approach with (i) standard VAE and (ii) Symmetric Equilibrium learning (Flach et al., 2024). The comparison with these works is only possible on a task with two groups of variables. We decided on conditional image generation on Fashion MNIST and CelebA datasets. The goal is to learn a joint model $p(x, z | c)$. It consists of a decoder $p(x | z, c)$ and an encoder $q(z | x, c)$, where x are images, c are classes or attributes, and z are the latent variables. For VAE and Symmetric learning, we additionally assume a particular fixed $p(z)$, hence $p(x, z | c) = p(z)p(x | z, c)$. In our approach, $p(x, z | c)$ is implicitly defined by the decoder and the encoder; i.e. we have no explicit assumption about the prior $p(z)$. All compared methods use the same architecture of the encoder and decoder, similar to Sections 5.3 and 5.4. For Fashion MNIST, we used binary latent z distributed a priori uniformly (for the first two methods). For CelebA, z are continuous with a Gaussian prior.

For each method and dataset, we report FID scores for (i) images generated from random codes, and (ii) images generated from the limiting distribution of the corresponding MCMC. The results are summarized in Table 1. The model for FMNIST images can combine good generative capabilities with consistency. Images generated from the limiting distribution are better than those generated from random codes, and our method gives the best FID score. However, this does not hold for the complex distribution of CelebA images. Good decoders in the considered model have no consistent encoder counterparts. Directed models (VAE, symmetric) focus on the decoder performance and achieve better FID scores when generating from random codes at the cost of consistency, which is, however, important for general inference tasks (as discussed in Section 4). Our method enforces more consistency and achieves less good

FID scores; however, it is still better than those from the limiting distribution of the directed models. Combining good generative capabilities with consistency requires more complex models, as e.g. the one used in the previous section. See Section D.2 for more discussion.

6. Conclusion

We consider deep multivariate models for heterogeneous collections of random variables and propose to model them in terms of conditional distributions for each variable conditioned on the rest. Learning such collections of conditional distributions can be approached as training a parametrised Markov chain kernel by maximising the data likelihood of its limiting distribution. This has the advantage of allowing a wide range of semi-supervised learning scenarios. Our training algorithm is not restricted to models with detailed balance because the choice of the (average) length of the sampling chain provides a means of balancing the bias towards detailed balance and the data likelihood objective.

Our experiments show that such models can be learned for simple and complex visual data. Particularly, we focus on the versatility of the learned models w.r.t. different inference tasks. Moreover, we show that once trained, they can be easily extended for more complex downstream tasks. Section D discusses limitations and open questions.

References

Arnold, B. C. and Strauss, D. J. Bivariate distributions with conditionals in prescribed exponential families. *Journal of the Royal Statistical Society Series B (Methodological)*, 53(2):365–375, 1991.

Arnold, B. C., Castillo, E., and Sarabia, J. M. Conditionally specified distributions: An introduction. *Statistical Science*, 16(3):249 – 274, 2001.

Besag, J. Statistical analysis of non-lattice data. *Journal of the Royal Statistical Society. Series D (The Statistician)*, 24(3):pp. 179–195, 1975.

Flach, B., Schlesinger, D., and Shekhovtsov, A. Symmetric equilibrium learning of VAEs. In *AISTATS*, volume 238, pp. 3214–3222, 2024.

Hinton, G. E. Products of experts. In *Artificial Neural Networks, 1999. ICANN 99. Ninth International Conference on (Conf. Publ. No. 470)*, volume 1, pp. 1–6. IET, 1999.

Hinton, G. E., Dayan, P., Frey, B. J., and Neal, R. M. The “Wake-Sleep” Algorithm for Unsupervised Neural Networks. *Science*, 268(5214):1158–1161, May 1995.

Ho, J., Jain, A., and Abbeel, P. Denoising diffusion probabilistic models. In Larochelle, H., Ranzato, M., Hadsell,

R., Balcan, M., and Lin, H. (eds.), *Advances in Neural Information Processing Systems*, volume 33, pp. 6840–6851. Curran Associates, Inc., 2020.

Kingma, D. P. and Welling, M. Auto-encoding variational bayes. In *ICLR*, 2014.

Kingma, D. P., Rezende, D. J., Mohamed, S., and Welling, M. Semi-supervised learning with deep generative models. In *NeurIPS*, NIPS’14, pp. 3581–3589, 2014.

Lamb, A., Hjelm, R. D., Ganin, Y., Cohen, J. P., Courville, A., and Bengio, Y. GibbsNet: Iterative adversarial inference for deep graphical models. In *NeurIPS*, pp. 5095–5104, 2017.

Liu, C., Tang, H., Qin, T., Wang, J., and Liu, T.-Y. On the generative utility of cyclic conditionals. In *NeurIPS*, 2021.

Rezende, D. J., Mohamed, S., and Wierstra, D. Stochastic backpropagation and approximate inference in deep generative models. In *ICML*, 2014.

Rombach, R., Blattmann, A., Lorenz, D., Esser, P., and Ommer, B. High-resolution image synthesis with latent diffusion models. In *CVPR*, pp. 10684–10695, 2022.

Seitzer, M. pytorch-fid: FID Score for PyTorch. <https://github.com/mseitzer/pytorch-fid>, August 2020. Version 0.1.1.

Shekhovtsov, A., Schlesinger, D., and Flach, B. VAE approximation error: ELBO and exponential families. In *The Tenth International Conference on Learning Representations, ICLR 2022, Virtual Event, April 25-29, 2022*. OpenReview.net, 2022.

Sohn, K., Lee, H., and Yan, X. Learning structured output representation using deep conditional generative models. In Cortes, C., Lawrence, N., Lee, D., Sugiyama, M., and Garnett, R. (eds.), *Advances in Neural Information Processing Systems*, volume 28. Curran Associates, Inc., 2015.

Tomczak, J. and Welling, M. VAE with a VampPrior. In *AISTATS*, pp. 1214–1223, January 2018.

Welling, M., Rosenzvi, M., and Hinton, G. E. Exponential family harmoniums with an application to information retrieval. In Saul, L., Weiss, Y., and Bottou, L. (eds.), *Advances in Neural Information Processing Systems*, volume 17. MIT Press, 2004.

A. Proofs and Examples

A.1. Proofs for the Generic Algorithm

The following result is a direct analogue of ELBO decomposition, applied to our recurrent lower bound.

Proposition 3.1. *The lower bound (4) has an equivalent reformulation $L_B(\theta, q, n) =$*

$$L(\theta) - n \sum_{x \in \mathcal{X}} Q_n(x) D_{KL}(q(x' | x) \| p_\theta^r(x' | x)), \quad (5)$$

where $p_\theta^r(x' | x) = p_\theta(x | x') p_\theta(x') / p_\theta(x)$ is the transition kernel of the reverse Markov chain.

Proof. We use the equality

$$\log p_\theta(x | x') = \log p_\theta^r(x' | x) - \log p_\theta(x') + \log p_\theta(x)$$

to substitute $\log p_\theta(x | x')$ in

$$L_B(\theta, q, n) = \sum_{x \in \mathcal{X}} q_{n+1}(x) \log p_\theta(x) + n \sum_{x, x' \in \mathcal{X}} q(x' | x) Q_n(x) [\log p_\theta(x | x') - \log q(x' | x)]. \quad (12)$$

Expanding terms we obtain

$$L_B(\theta, q, n) = \sum_x [q_{n+1}(x) + n Q_n(x)] \log p_\theta(x) - \quad (13)$$

$$n \sum_{x, x'} q(x | x') Q_n(x') \log p_\theta(x) - n \sum_x Q_n(x) D_{KL}(q(x' | x) \| p_\theta^r(x' | x)). \quad (14)$$

Recalling the definition

$$q_k(x) = \sum_{x' \in \mathcal{X}} q(x | x') q_{k-1}(x') \quad (15)$$

$$Q_n(x) = \frac{1}{n} \sum_{k=1}^n q_k(x). \quad (16)$$

it is easy to prove that the first two terms collapse to the data likelihood

$$L(\theta) = \sum_{x \in \mathcal{X}} q(x) \log p_\theta(x). \quad (17)$$

□

Proposition 3.2. *Let $q(x' | x)$ be such that its unique limiting distribution coincides with $p_{\bar{\theta}}(x)$ for a given fixed $\bar{\theta}$. Then the gradient of the first term of (4) in θ at $\bar{\theta}$ asymptotically vanishes for $n \rightarrow \infty$. In particular, it holds that $\|\nabla_\theta \sum_{x \in \mathcal{X}} q_n(x) \log p_\theta(x)\|_1 \leq C \alpha^n$ with some $\alpha \in (0, 1)$ related to the mixing time of the kernel $q(x' | x)$ and a positive constant C .*

Proof. If the Markov chain with kernel $q(x | x')$ has the limiting distribution $p_{\bar{\theta}}(x)$, then by construction $q_n(x)$ converges to this distribution. It follows that the first term in (4) converges to

$$\sum_{x \in \mathcal{X}} q_{n+1}(x) \log p_\theta(x) \xrightarrow{n \rightarrow \infty} \sum_{x \in \mathcal{X}} p_{\bar{\theta}}(x) \log p_\theta(x), \quad (18)$$

Its gradient for $q_\infty(x) = p_{\bar{\theta}}(x)$ expresses as

$$\begin{aligned} \nabla_\theta \sum_{x \in \mathcal{X}} p_{\bar{\theta}}(x) \log p_\theta(x) &= \sum_{x \in \mathcal{X}} p_{\bar{\theta}}(x) \nabla_\theta \log p_\theta(x) \\ &= \sum_{x \in \mathcal{X}} p_{\bar{\theta}}(x) \frac{1}{p_{\bar{\theta}}(x)} \nabla_\theta p_\theta(x) = \sum_{x \in \mathcal{X}} \nabla_\theta p_\theta(x) = \nabla_\theta \sum_{x \in \mathcal{X}} p_\theta(x) = \nabla_\theta 1 = 0. \end{aligned}$$

Moreover, we can bound the norm of the gradient for finite n by

$$\left\| \nabla_{\theta} \sum_{x \in \mathcal{X}} q_n(x) \log p_{\theta}(x) \right\|_1 = \left\| \sum_{x \in \mathcal{X}} [q_n(x) - p_{\bar{\theta}}(x)] \nabla_{\theta} \log p_{\theta}(x) \right\|_1 \leq \|q_n - p_{\bar{\theta}}\|_{TV} \max_{x \in \mathcal{X}} \|\nabla_{\theta} \log p_{\theta}(x)\|_1. \quad (19)$$

The claim is then a direct consequence of the convergence of q_n to its limiting distribution, being equal $p_{\bar{\theta}}$. This convergence is geometric: $\|q_n - p_{\bar{\theta}}\|_{TV} \leq \tilde{C} \alpha^n$, where $\alpha \in (0, 1)$ depends on the mixing time of the kernel $q(x' | x)$. The constant C is then equal to $\tilde{C} \max_{x \in \mathcal{X}} \|\nabla_{\theta} \log p_{\theta}(x)\|_1$ at $\theta = \bar{\theta}$. \square

A.1.1. FURTHER USED FACTS

The expression for the gradient estimate (6) is obtained as follows. Let us expand the gradient of the second term of (4), i.e. of

$$\hat{F} = n \sum_{x, x' \in \mathcal{X}} q(x' | x) Q_n(x) \left[\log p_{\theta}(x | x') - \log q(x' | x) \right]. \quad (20a)$$

Since q is not varied with θ , the gradient of $\log q(x' | x)$ is zero. Substituting $Q_n(x) = \frac{1}{n} \sum_{k=1}^n q_k(x)$ we obtain

$$\nabla_{\theta} \hat{F} = \sum_{x, x' \in \mathcal{X}} q(x' | x) \sum_{k=1}^n q_k(x) \nabla_{\theta} \log p_{\theta}(x | x') = \sum_{k=1}^n \sum_{x, x' \in \mathcal{X}} q(x' | x) q_k(x) \nabla_{\theta} \log p_{\theta}(x | x'). \quad (21)$$

If we sample $x^1 \sim q_1(x)$, $x^{k+1} \sim q(x' | x^k)$, then (x^{k+1}, x^k) is a sample from $q(x' | x) q_k(x)$. Therefore, g in (6) is an unbiased stochastic gradient estimate of \hat{F} .

The fact that the reverse chain has the same limiting distribution as the forward one is verified as follows. We have by definition

$$p_{\theta}^r(x' | x) = p_{\theta}(x | x') p_{\theta}(x') / p_{\theta}(x)$$

and

$$p_{\theta}(x) = \sum_{x'} p_{\theta}(x') p_{\theta}(x | x').$$

We substitute and verify that

$$\sum_x p_{\theta}(x) p_{\theta}^r(x' | x) = \sum_x p_{\theta}(x) p_{\theta}(x | x') p_{\theta}(x') / p_{\theta}(x) = \sum_x p_{\theta}(x | x') p_{\theta}(x') = p_{\theta}(x'). \quad (22)$$

A.2. Proof of the Theorem

First, we recall our setup. We consider a collection of conditional distributions $p_{\theta_i}(x_i | x_{-i})$, $i = 1, \dots, m$, where x_i is a particular variable from $x = (x_1, x_2 \dots x_m)$, and x_{-i} summarises all variables except x_i . The Markov kernel of the corresponding MCMC process is defined as

$$p_{\theta}(x | x') = \sum_{i=1}^m \alpha_i p_{\theta_i}(x_i | x_{-i}) \mathbb{I}[x_{-i} = x'_{-i}], \quad (23)$$

and its limiting distribution is denoted by $p_{\theta}(x)$. The stationarity condition for this kernel implies that its limiting distribution has the form of a mixture

$$p_{\theta}(x) = \sum_{i=1}^m \alpha_i p_{\theta_i}(x_i | x_{-i}) p_{\theta}(x_{-i}). \quad (24)$$

It is not necessarily the case that *limiting conditionals* $p_{\theta}(x_i | x_{-i})$ coincide with the *model conditionals* $p_{\theta_i}(x_i | x_{-i})$.

We call a collection of conditional distributions *consistent* if there exists a joint distribution having them as conditionals.

Theorem 4.2. *The Markov chain defined by the kernel (7) satisfies detailed balance if and only if the collection of conditional distributions $p_{\theta_i}(x_i | x_{-i})$, $i = 1, \dots, m$ is consistent. In this case, all individually modelled conditionals $p_{\theta_i}(x_i | x_{-i})$ coincide with the corresponding conditionals of the limiting distribution, $p_{\theta}(x_i | x_{-i})$.*

Proof. We begin the proof with the last statement. If the conditionals of the stationary distribution coincide with the model conditionals, then the latter are consistent with the joint being $p_\theta(x)$.

If the model conditionals $p_{\theta_i}(x_i | x_{-i})$ are consistent, i.e. have a common joint $\bar{p}(x)$, then the MCMC with the kernel (23) is a standard Gibbs sampler for $\bar{p}(x)$, its limiting distribution is $\bar{p}(x) = p_\theta(x)$, and its limiting conditionals are $\bar{p}(x_i | x_{-i}) = p_\theta(x_i | x_{-i}) = p_{\theta_i}(x_i | x_{-i})$. In this case, the mixture (24) does not depend on the weights α_i because all its components coincide. The standard Gibbs sampler is also known to satisfy the detailed balance.

It remains to prove the reverse, i.e. assuming detailed balance for the MCMC kernel (23), we prove that the collection of conditionals is consistent. Let us consider a particular x_i , its complement x_{-i} , and the corresponding conditional $p_{\theta_i}(x_i | x_{-i})$. We aim at proving $p_{\theta_i}(x_i | x_{-i}) = p_\theta(x_i | x_{-i})$. The detailed balance constraint expressed in these components reads

$$p_\theta(x_i, x_{-i}) \cdot p_\theta(x'_i, x'_{-i} | x_i, x_{-i}) = p_\theta(x'_i, x'_{-i}) \cdot p_\theta(x_i, x_{-i} | x'_i, x'_{-i}). \quad (25)$$

Recall that our kernel (23) has the property that in each transition either x_{-i} or x_i can change but not both simultaneously.

In the former case, $x_{-i} \neq x'_{-i}$, the i -th addend in (23) is zero for any (x, x') due to the vanishing indicator $\llbracket x_{-i} = x'_{-i} \rrbracket$. So, we can not draw any conclusion about p_{θ_i} from (25).

Let us consider the latter case $x_{-i} = x'_{-i}$. If $x_i = x'_i$, the left-hand side and the right-hand side of (25) are equal for any (x, x') . Hence, again we can not draw any conclusion about p_{θ_i} from (25).

It remains only to consider the case $x_{-i} = x'_{-i}$ and $x_i \neq x'_i$. We substitute (23) into (25). All addends in the sum of (23) except the i -th one vanish (as the corresponding indicators are zero). The factor α_i on both sides cancels. Therefore, (25) is reduced to

$$p_\theta(x_i, x_{-i}) \cdot p_{\theta_i}(x'_i | x_{-i}) = p_\theta(x'_i, x_{-i}) \cdot p_{\theta_i}(x_i | x_{-i}), \quad (26)$$

or, equivalently

$$p_\theta(x_i | x_{-i}) \cdot p_{\theta_i}(x'_i | x_{-i}) = p_\theta(x'_i | x_{-i}) \cdot p_{\theta_i}(x_i | x_{-i}). \quad (27)$$

It follows

$$\frac{p_{\theta_i}(x_i | x_{-i})}{p_{\theta_i}(x'_i | x_{-i})} = \frac{p_\theta(x_i | x_{-i})}{p_\theta(x'_i | x_{-i})} \quad \forall x_i, x'_i, x_{-i}, \quad (28)$$

which finally means $p_{\theta_i}(x_i | x_{-i}) = p_\theta(x_i | x_{-i})$. As $p_\theta(x_i | x_{-i})$ are consistent per definition with the joint being $p_\theta(x)$, so are also $p_{\theta_i}(x_i | x_{-i})$.

□

A.3. Examples

We mentioned in Remark 3.4 that denoising diffusion is a prominent example showing that a linearly growing gap between the likelihood and the lower bound in (5) does not necessarily lead to a breakdown of the approach.

Example 1. Denoising diffusion (Ho et al., 2020; Rombach et al., 2022) fixes $q(x | x')$ to a simple ‘‘noisifying’’ model, whose limiting distribution is independent standard Gaussian noise, i.e. $\lim_{n \rightarrow \infty} q_n = \mathcal{N}(0, \mathbb{I})$.⁵ This has the advantage, that the distributions $q_n(x)$ can be computed in closed form. The disadvantage of the diffusion approach is that the lower bound is no longer tight and the corresponding gap increases linearly with the sampling length. This follows from (5) because the KL-divergence $D_{KL}(q(x' | x) \parallel p_\theta^r(x' | x))$ is strictly positive since the limiting distributions of $p_\theta(x | x')$ and $q(x | x')$ are different by definition. Despite the convincing experimental results, it remains unclear whether the method maximises the true objective function, i.e. the data likelihood, when maximising the lower bound with the chosen fixed diffusion process.

The next examples show that the proposed Algorithm 1 is similar to known techniques in simple cases.

Example 2. Consider the supervised case, i.e. with complete realisations $x = (x_1, x_2 \dots x_m)$. If we stop the reverse chain at $n = 1$, the optimised objective becomes

$$L_P(\theta) = \frac{1}{m} \sum_{i=1}^m \log p_{\theta_i}(x_i | x_{-i}) + \text{const}, \quad (29)$$

⁵We consider a slightly simplified version of the diffusion model, assuming that both, the forward and reverse processes are homogeneous Markov chains.

which corresponds to *pseudo-likelihood* (Besag, 1975). Notice that this enforces consistency simply because the empirical data distribution has by itself consistent conditionals.

Example 3. Let us consider the task of learning an EF-Harmonium (Welling et al., 2004)

$$p_W(x, y) = \frac{1}{Z(W)} \exp\langle \psi(x), W\xi(y) \rangle, \quad (30)$$

with sufficient statistics ψ and ξ , in the fully supervised case. A stochastic gradient of $\log p_W(x | y)$ can be obtained with

$$\hat{x} \sim p_W(x | y), \quad (31a)$$

$$\hat{\nabla}_W \log p_W(x | y) = \psi(x) \otimes \xi(y) - \psi(\hat{x}) \otimes \xi(y). \quad (31b)$$

The gradient of $\log p_W(y | x)$ is similar. This model is consistent by design and the sampler (7) satisfies detailed balance. Applying the proposed learning algorithm results in the *contrastive divergence* algorithm (Hinton, 1999). This is because almost all gradient terms for the sequence $((x_1, y_1), \dots, (x_n, y_n))$ sampled from (7) cancel out, which leaves the gradient estimated for the chain as

$$g = \psi(x_1) \otimes \xi(y_1) - \psi(\hat{x}_n) \otimes \xi(\hat{y}_n). \quad (32)$$

B. Validation Experiments: Dependency on the Chain Length

We present additional details and further experiments accomplishing results from Sec. 5.2

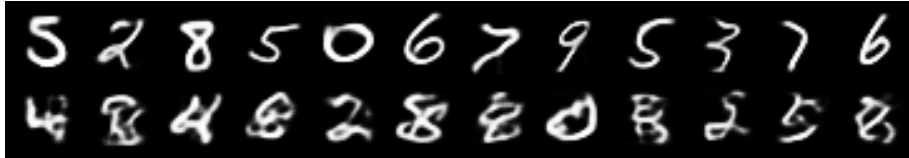


Figure 6. Given a code z , images are obtained by sampling, which alternates between sampling from $p(x | c, z)$ and $p(c | x, z)$, i.e. $x \sim p(x | z)$. Top row: $z \sim \pi(z)$ (see the text), bottom row: z uniform.

We used the marginal distribution $p(z)$ from our MNIST experiments as the target probability distribution $\pi(z)$. Recall that in the MNIST experiments we learned three conditional probability distributions $p(x | c, z)$, $p(c | x, z)$ and $p(z | x, c)$, where x are binarised MNIST images, c are classes (digits), and z are binary latent variables. The trained model admits sampling from $\pi(z)$ as follows: (i) pick an example (x, c) from the MNIST training set, and (ii) sample $z \sim p(z | x, c)$. Fig. 6 illustrates that the obtained $\pi(z)$ is not trivial.

In Section 5.2 we presented a dependency of the model consistency (addressed implicitly through the matrix symmetry) on the chain length for a simple log-linear model (10). Here we present a more detailed view, i.e. we want to inspect the dependency of the optimisation objective on n during training. However, when defining the generic algorithm, we have omitted an intractable term $\sum_x q_{n+1}(x) \log p_\theta(x)$, which has an asymptotically vanishing gradient but a non-negligible value. In order to approximate the value of $L_B(\theta, q, n)$ more accurately we use the objective

$$F(\theta, q, n) = \sum_{x, x' \in \mathcal{X}} q(x' | x) q_n(x) \log q(x' | x) + n \sum_{x, x' \in \mathcal{X}} q(x' | x) Q_n(x) \left[\log p_\theta(x | x') - \log q(x' | x) \right], \quad (33)$$

see Section B.1 for the rationale.

We perform three experiments:

1. Using log-linear transition probability (10).
2. Recall that (10) satisfies detailed balance iff the matrix W is symmetric. In the second experiment we enforce detailed balance by setting $W = \frac{1}{2}(W + W^T)$ after each update iteration.
3. Instead of the log-linear form (10) we use an MLP for $p(z_t | z_{t-1})$ having one hidden layer with 128 units and tanh-activations.

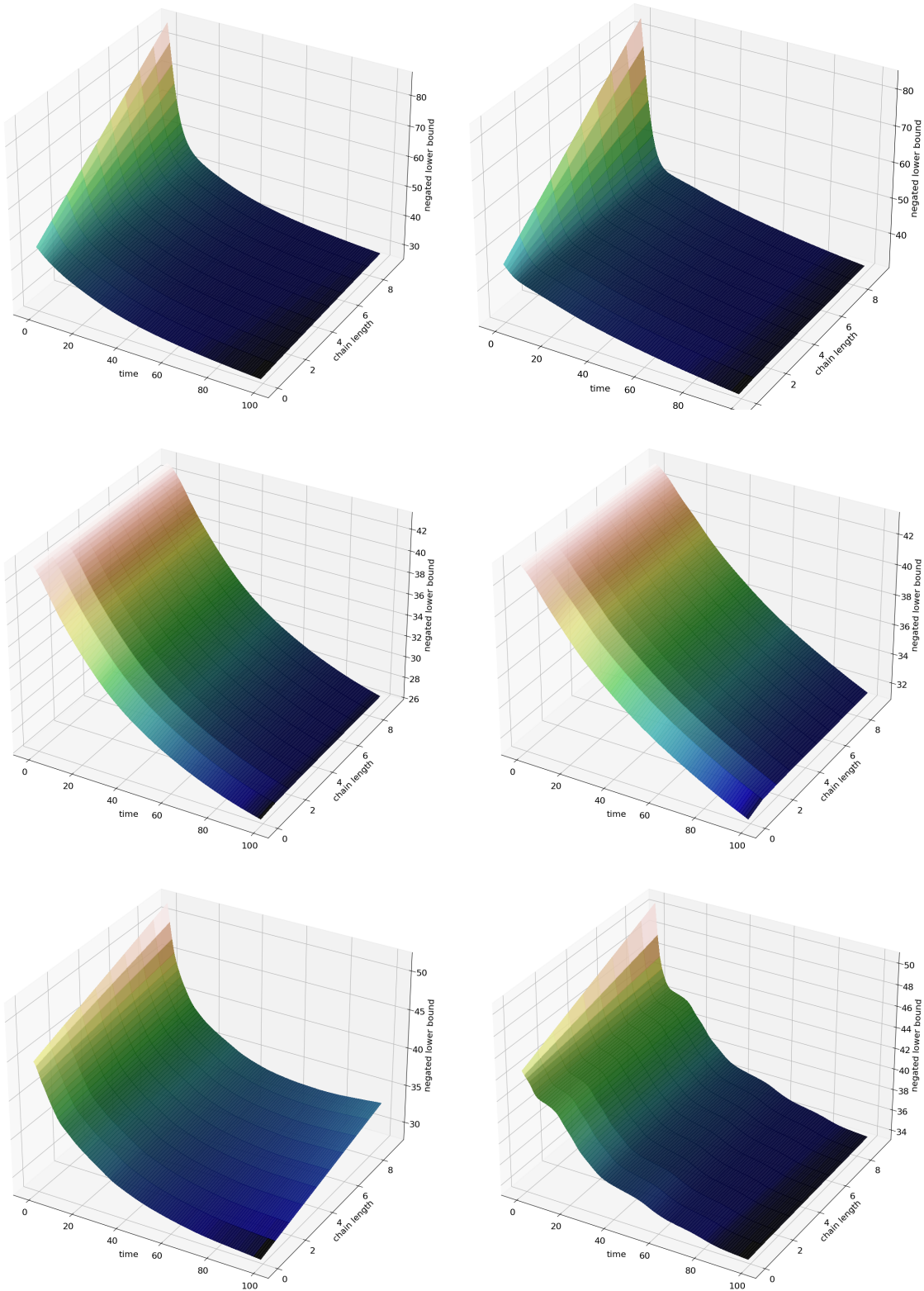


Figure 7. The dependencies of the optimisation objective on the chain length during the training. Top row: log-linear model, second row: symmetrised log-linear model, bottom row: MLP. Left: short optimisation chains, right: long optimisation chains.

For each of these three cases we perform the learning two times. First with short chains, using $n = 1$, and second with longer chains, using $n = 10$.

The results are presented in Fig. 7. For both optimizing with $n = 1$ and optimizing with $n = 10$, we plot the values of the objective (33) for all n -s in dependency on the training time. The results confirm our expectations. When detailed balance is not explicitly enforced (experiments (1) and (3)), the objective grows linearly with n at the beginning of the learning, i.e. when the parameters are randomly initialised, and hence, the details balance is not satisfied. As conjectured, our algorithm implicitly enforces detailed balance, i.e. the graphs are almost horizontal along the n -direction at the end of the learning process. Sometimes, if detailed balance is “easy to achieve” (the first experiment), short chains enforce detailed balance almost as good as long ones. In general, however, enforcing detailed balance requires longer chains (see experiment (3)). Finally, if detailed balance is satisfied by design (experiment (2)), the graphs are horizontal along the n -direction from the very beginning. In this case, short and long chains work equally good.

B.1. Approximating the value of LB

A natural choice of approximating $L_B(\theta, q, n)$ would be just to drop the intractable term $\sum_x q_{n+1}(x) \log_\theta(x)$, i.e., to approximate L_B as

$$\hat{F}(\theta, q, n) = n \sum_{x, x' \in \mathcal{X}} q(x' | x) Q_n(x) \log \frac{p_\theta(x | x')}{q(x' | x)}. \quad (34)$$

However, even when the gradient of this omitted term asymptotically vanishes for $n \rightarrow \infty$, its value does not. It is asymptotically the value of the entropy of $p_\theta(x)$. To approximate it a bit better we add back a tractable averaged conditional entropy of q , which results in the approximation

$$F(\theta, q, n) = \sum_{x, x' \in \mathcal{X}} q(x' | x) q_n(x) \log q(x' | x) + n \sum_{x, x' \in \mathcal{X}} q(x' | x) Q_n(x) \log \frac{p_\theta(x | x')}{q(x' | x)} \quad (35)$$

(see (33)). We can formally show the following.

Proposition B.1. *For discrete variables, asymptotically for $n \rightarrow \infty$, F (35) is a better approximation of the lower bound (4) than \hat{F} (34).*

Proof. Consider $q(x' | x) = p_\theta(x' | x)$ and θ fixed. In the limit $n \rightarrow \infty$, $q_n(x)$ approaches $p_\theta(x)$ (see proof of Proposition 3.2 above). Then, for \hat{F} , the approximation can be expressed as

$$\hat{F}(n) - L_B(n) \rightarrow - \sum_x q_n(x) \log q_n(x), \quad (36)$$

which is the entropy H of $q_n(x)$. For discrete variables, H is non-negative and therefore \hat{F} is asymptotically an overestimate of L_B .

For F , we obtain

$$F(n) - L_B(n) \rightarrow \sum_{x, x'} q_n(x, x') \log \frac{q_n(x, x')}{q_n(x) q_n(x')}, \quad (37)$$

which is the mutual information I between x and x' drawn from $q_n(x, x') = q_n(x' | x) q_n(x)$. Since I is non-negative, this shows that F also asymptotically overestimates L_B .

There holds $H \geq I$ because their difference $H - I$ is the averaged conditional entropy, which is non-negative for discrete variables. It follows that asymptotically

$$L_B \leq F \leq \hat{F} \quad (38)$$

and hence F is more accurate.

We also obtained the following interpretation of the approximation F : it is (asymptotically) accurate when the chain has weak coupling (mutual information between consecutive states is small), i.e. when it mixes fast. \square

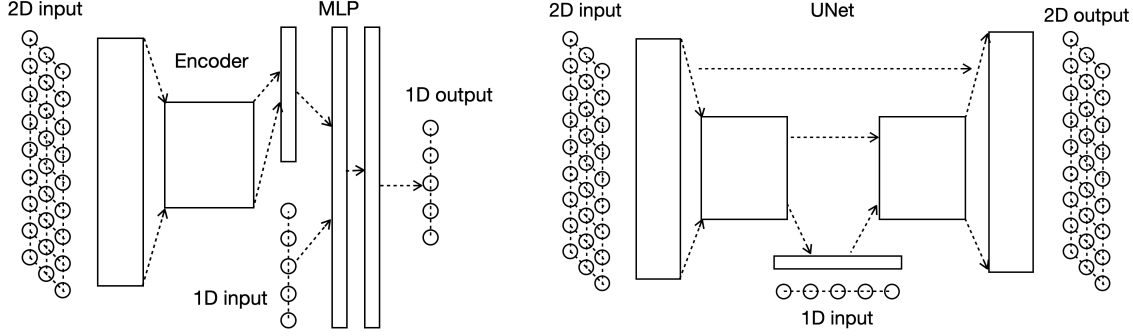


Figure 8. Network architectures. Left: for 1D outputs, right: for 2D outputs.

C. Network Architectures

Here we describe network architectures used in our experiments. We focus on those used for CelebA in section 5.4. Models for MNIST and Fashion MNIST consist of very similar building blocks.

In CelebA, we have two types of networks. The first one, shown in Fig. 8 (left), gets both 1D and 2D inputs and produces a 1D output, for example $p(y | c, x, z, s)$. Thereby, several 1D inputs are concatenated, 2D inputs are concatenated along the channel direction. First, the 2D input goes through an encoder-like network, i.e. a convolutional network of decreasing spatial resolution. The encoder consists of 9 convolutional layers. Some of them are performed with strides, effectively reducing spatial resolution. The output of the encoder is a feature vector, which is then concatenated with the 1D input. The resulting vector goes through an MLP consisting of 3 fully connected layers. The output values are interpreted according to the used output type, i.e. for which component they are used. For attributes c and binary latent variables y , the network outputs the corresponding logits. For continuous output z , it provides components means and logarithms of the variances.

The second network type, shown in Fig. 8 (right), gets again both 1D and 2D inputs, but produces a 2D output, e.g. $p(s | c, x, y, z)$. It has a UNet-like architecture, i.e. it consists of an encoder and a decoder, equipped with additional skip-connections. The encoder is of the same architecture as for the first network type, the decoder has the inverse architecture, i.e. the same number of layers, hidden units, etc., using, however, transposed convolutions. The 1D input is concatenated to the UNet's hidden layer of the lowest, i.e. 1×1 , resolution.

We used the Adam optimiser with a gradient step size $1e-4$ in all our experiments. Further details can be found in the source code, which will be made available upon publication.

D. Discussion and Limitations

D.1. Computational Time and Scalability

Inference: The inference in one of the directly modelled directions is naturally fast. For general inference problems, where MCMC sampling is required, we may speak, without loss of generality, about the time for unclamped generation because clamping on some data can be expected to make the mixing time only faster. The MCMC mixing time is critical in this case. It, however, depends on the model design and how it is learned. Currently, we do not have control of the mixing time and focus on the training methodology and proof-of-concept experiments. For qualitative results, we used 1000 MCMC steps. In this setting, generation with the CelebA model in Section 5.4 is accomplished in under a second on NVIDIA TITAN Xp GPU (for one example or a batch of examples in parallel). For quantitative (FID) evaluation, we used 100 MCMC steps. When the generation is done in batches, generating 30K images took about half an hour. Overall, we used a conservatively high number of steps acceptable for us to perform the experiments. At the same time, we believe it might be possible to achieve models with both the desired limiting distribution and a fast mixing. In general, we consider the proposed limiting distribution model to be in the same computational complexity “weight category” as, e.g. diffusion models.

Learning: Note that the proposed implementation of the algorithm blends learning and the recurrent lower bound expansion. Completion of new samples by MCMC in step 1 does not need backprop, and new samples are only needed for a fraction of the training batch at each training iteration, so the MCMC cost gets amortised. However, the current implementation

performs completion and training sequentially, and we used only 10 sampling iterations for completion. The training time was then dominated by the blended training step (executed for a batch of data with backpropagation). We also used a conservatively small learning rate, an average chain length of 16, and a long training duration (1000 epochs). The learning of CelebA then took quite long indeed, about 4 days on a single NVIDIA H100 GPU. Learning simpler models, like we used for MNIST, takes several hours.

On the other hand, completing the samples can in principle run in parallel to training, possibly caching completed data so that it would not slow down training even if with many MCMC steps. The total computation cost of our approach, per blended learning step, can therefore be made linear in the total number of model parameters regardless of the number of groups of variables (and it is standardly linear in other meta-parameters such as batch size, etc.). The dimensionality of the data does not have a substantial impact. We thus propose that scalability is not a principled limitation for a moderate chain length n .

D.2. Discussion of the Results in Table 1

First, we note that the experimental setup is a direct comparison using exactly the same decoder and encoder architectures for all three methods, selected so that none of the methods fail due to their potential weaknesses (e.g. posterior collapse for VAE).

Compared to VAE and Symmetric in this setup, our approach lifts the assumption of a factorised (Bernoulli / Gaussian) prior. This potentially makes the model more flexible to learn a complex distribution of latent variables. On the other hand, it enforces more consistency (as the analysis of the recurrent lower bound and the synthetic experiment show). Consistency can be rather restrictive in this setting with two conditionals factorising over output’s coordinates. Note that the limitation to two groups of variables is necessary to enable a direct comparison. For FMNIST, this does not appear to be too restrictive and we observe a better quality of the limiting distribution than the baselines using single-sample or limiting. For CelebA, while our more advanced model in Section 5.4 can circumvent these restrictions by using more groups of variables, the two-groups model here can not. We observe that enforcing consistency in this case is at the expense of the modelling power and the basic VAE in this case is better and faster for the generation task. At the same time, consistency is desired for other possible inference tasks. The “limiting” evaluation in Table 1 can be viewed as a surrogate of such tasks as it depends on both the model fit and consistency. The evidence “Ours > Symmetric > VAE” in the limiting evaluation for both MNIST and CelebA supports a better utility for general inference tasks.

We further argue that consistency is more important for more complex models with several groups of variables (e.g. images, segmentations, and attributes). If the inference task is complex (e.g. we want to infer several groups of variables) and not known in advance or there is no fully labelled data for that task, consistency is essential. The proposed approach can control (at least in theory) the trade-off between the data likelihood and consistency by varying the chain length.

D.3. Chain length

As we have discussed, the chain length n is a meta-parameter of the learning algorithm that controls the trade-off between the data likelihood and the consistency of the learned conditionals. A longer chain length enforces more consistency. It also affects the quality of the approximation of the gradient of the data likelihood. A longer chain length provides a better approximation. It is therefore desirable to better understand its impact in dependence of the data complexity, the expressive power of the chosen model class as well as of the subset of models with detailed balance.

In our experiments, we used a fixed chain length during the whole training. We have not yet experimented with varying it during the training. It might indeed be desirable to start the learning with short (expected) chain lengths and then gradually increase the length when progressing with learning. A possible argument is that even an approximation of the gradient of $L_B(\theta, g, n)$ for small n is sufficient to improve the data likelihood at the beginning of the training, when the current model is still far from the optimal one. On the other hand, if it is already close, then a better approximation of the gradient is needed, which is achieved by a longer chain length.